5.2.1 Oscillating cylinder in inviscid fluid

Because oscillating cylinder experiments are performed typically in salt-stratified fluid, we assume the fluid is Boussinesq and uniformly stratified with (constant) buoyancy frequency N_0, given by (3.2). We suppose the cylinder has a circular cross-section with radius a and that it oscillates vertically up and down at frequency ω. The amplitude of its oscillation (half the peak-to-peak vertical displacement) is denoted by A; the maximum vertical velocity is $W = A\omega$.

We will not look at the transient start-up problem here. Instead, we will assume the cylinder has been oscillating for such a long time that the fluctuation fields themselves oscillate at frequency ω everywhere in space. We do not expect the disturbances to have any structure in the y-direction, which is parallel to the cylinder axis. Thus we can represent the fluid motion in terms of the streamfunction by

$$\psi(x,z,t) = \Psi(x,z)e^{-\imath\omega t}. \tag{5.1}$$

Here $\Psi(x,z)$ is the possibly complex-valued 'streamfunction amplitude' and it is understood that the actual streamfunction is the real part of (5.1). The magnitude of the streamfunction amplitude $|\Psi|$ represents the streamfunction amplitude envelope. This is the maximum value of the streamfunction field at any point in space for all time.

Once Ψ is determined, the velocity field is given by (the real parts of)

$$u = -\frac{\partial \Psi}{\partial z}e^{-\imath\omega t} \quad \text{and} \quad w = \frac{\partial \Psi}{\partial x}e^{-\imath\omega t}. \tag{5.2}$$

We begin by neglecting the effects of viscosity, later including them to model beam attenuation. In inviscid fluid, we found that ψ satisfies the differential equation (3.40). Using (5.1), this gives an equation for the streamfunction amplitude:

$$N_0{}^2\frac{\partial^2 \Psi}{\partial x^2} - \omega^2\nabla^2\Psi = 0. \tag{5.3}$$

The boundary conditions require that the fluid on the boundary of the cylinder moves vertically with the speed of the cylinder. Taking the maximum vertical speed to be $W > 0$, the streamfunction on the cylinder is

$$\Psi|_C = Wx|_C = -Wa\sin(\theta). \tag{5.4}$$

Here the cylinder boundary $C = \left\{(x,z) \mid x^2 + z^2 = a^2\right\}$ is taken to be stationary, consistent with the assumption of small-amplitude oscillations, $A \ll a$. It follows from (5.2) that the actual vertical velocity on C at some time t is $\Re\{W\exp(-\imath\omega t)\} = W\cos(\omega t)$. So, with $W > 0$, $t = 0$ corresponds to the time at which the cylinder moves upwards through its equilibrium position.

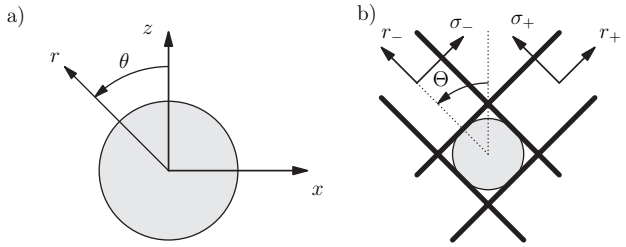

Fig. 5.1. a) Co-ordinate system used to model potential flow around a cylinder and b) the co-ordinate system used to model the across-beam ($\sigma_\pm$) and along-beam ($r_\pm$) axes.

The second expression in (5.4) has been recast in polar co-ordinates with θ being taken counter-clockwise from the z-axis, as shown in Figure 5.1a. We also impose the condition that the waves either vanish far from the cylinder if $\omega > N_0$, or that energy is transported away from the cylinder if $\omega < N_0$.

Before solving the boundary value problem explicitly, we examine the solution in the case $N_0 = 0$, corresponding to the disturbance field that arises in uniform-density fluid. In this case, (5.3) reduces to the potential equation

$$\nabla^2 \Psi = 0. \tag{5.5}$$

The general solution may be found through the method of separation of variables invoked in cylindrical co-ordinates. Requiring vanishing solutions for large r, we have

$$\Psi(r,\theta) = \sum_{n=1}^{\infty} r^{-n} \left[A_n \cos(n\theta) + B_n \sin(n\theta)\right] = \sum_{n=1}^{\infty} \mathcal{A}_n \mathcal{Z}^{-n} + \text{ cc}, \tag{5.6}$$

in which A_n and B_n are real constants. In the second expression we have recast the result in terms of the complex variable $\mathcal{Z} = \imath r e^{\imath\theta}$ using the polar co-ordinate system shown in Figure 5.2a. $\mathcal{A}_n$ are generally complex constants and cc denotes the complex conjugate of the sum.

Applying the boundary condition (5.4) written in polar co-ordinates, we see immediately that Ψ must satisfy

$$\Psi(r,\theta) = -W\frac{a^2}{r}\sin\theta = \frac{1}{2}W\frac{a^2}{\mathcal{Z}} + \text{ cc}. \tag{5.7}$$

This result is what we would get from solving the problem of irrotational flow around a cylinder translating at speed W. For the problem of the oscillating cylinder, the flow alternately moves upwards and downwards around the cylinder with frequency ω, as prescribed by the real part of the right-hand side of (5.1).

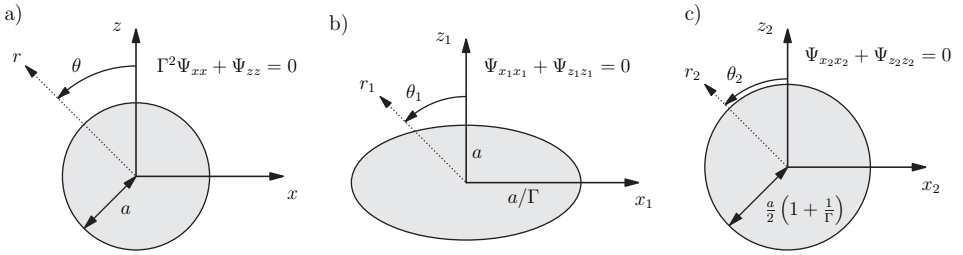

Fig. 5.2. a) Schematic illustrating the boundary value problem in x–z space, b) transformation to the potential equation and corresponding boundary in x_1–z_1 space and c) the corresponding boundary problem for flow around a cylinder in x_2–z_2 space determined under the Joukowski transformation.

Our plan first is to extend this result to the case $\omega > N_0$. This will likewise give a potential flow equation that can be solved by co-ordinate transformations involving the method of conformal mapping. Thereafter, by the method of analytic continuation, we will derive the expression for the streamfunction amplitude in the case $\omega < N_0$.

If $\omega > N_0$, (5.3) can be written

$$\Gamma^2 \frac{\partial^2 \Psi}{\partial x^2} + \frac{\partial^2 \Psi}{\partial z^2} = 0, \tag{5.8}$$

in which $\Gamma^2 \equiv 1 - {N_0}^2/\omega^2 > 0$. This is recast into the form of the potential equation (5.5) through the co-ordinate transformation $(x, z) = (\Gamma x_1, z_1)$. The corresponding boundary condition becomes

$$\Psi|_{C_1} = W\Gamma x_1\,|_{C_1} = W\Gamma \frac{a}{2\imath \exp(\imath\theta_1)} + \text{ cc.} \tag{5.9}$$

In the last expression, the transformed complex co-ordinate $\mathcal{Z}_1 \equiv x_1 + \imath z_1 = \imath r_1 e^{\imath\theta_1}$ has been evaluated on the elliptical boundary $C_1 = \left\{(x_1, z_1) \mid (\Gamma x_1)^2 + {z_1}^2 = a^2\right\}$. So the problem reduces to that of finding the potential flow around an ellipse centred at the origin with major axis a/Γ lying on the x-axis and minor axis a lying on the z-axis. The resulting boundary value problem is illustrated schematically in Figure 5.2b.

By the method of conformal mapping, we can transform the problem of potential flow around a cylinder of radius $a_2 = a(1 + 1/\Gamma)/2$ to that of flow around the ellipse C_1. This is done through the Joukowski transformation:

$$\mathcal{Z}_1 = \mathcal{Z}_2 + \frac{a^2}{4}\left(\frac{1}{\Gamma^2} - 1\right)\frac{1}{\mathcal{Z}_2}, \tag{5.10}$$

in which $\mathcal{Z}_2 \equiv x_2 + \imath z_2 = r_2 e^{\imath\theta_2}$ is the complex co-ordinate system in which the circular cylinder of radius a_2 centred at the origin is embedded. The resulting boundary value problem is illustrated schematically in Figure 5.2c. The inverse transform, found by solving the quadratic equation, is

$$\mathcal{Z}_2 = \frac{1}{2}\left[\mathcal{Z}_1 + \sqrt{{\mathcal{Z}_1}^2 + a^2\left(1 - \frac{1}{\Gamma^2}\right)}\right]. \tag{5.11}$$

It is straightforward to check that substituting the parametric representation of the ellipse $C_1 = \{\mathcal{Z}_1 = -(a/\Gamma)\sin\theta + \imath\, a\cos\theta \mid 0 \le \theta < 2\pi\}$ into (5.11) gives the circle $C_2 = \{\mathcal{Z}_2 = \imath a(1 + 1/\Gamma)/2 \exp(\imath\theta_2) \mid 0 \le \theta < 2\pi\}$.

From (5.10), we can write x_1 in terms of x_2 and so the boundary condition (5.9) on C_2 becomes

$$\Psi|_{C_2} = W\frac{2\Gamma}{\Gamma+1}x_2\bigg|_{C_2} = W\frac{\Gamma}{\Gamma+1}\,\frac{a_2}{\imath\exp(\imath\theta_2)} + \text{ cc}. \tag{5.12}$$

At this point we can use our solution for potential flow around a cylinder (5.7) and so find the streamfunction amplitude in the complex x_2–z_2 plane:

$$\Psi(\mathcal{Z}_2) = W\frac{\Gamma}{\Gamma+1}\frac{{a_2}^2}{\mathcal{Z}_2} + \text{ cc } = \frac{1}{4}W\left(1 + \frac{1}{\Gamma}\right)\frac{a^2}{\mathcal{Z}_2} + \text{cc} \tag{5.13}$$

for all $\mathcal{Z}_2$.

Using (5.11) to recast this result in terms of $\mathcal{Z}_1$ and then in terms of $\mathcal{Z} = (x/\Gamma) + \imath z$, we have

$$\Psi(x,z) = \frac{1}{2}Wa^2\left(1 + \frac{1}{\Gamma}\right)\left[\,\mathcal{Z} + \sqrt{\mathcal{Z}^2 + a^2(1 - 1/\Gamma^2)}\,\right]^{-1} + \text{ cc}. \tag{5.14}$$

Though algebraically complicated if written explicitly in terms of x and z, (5.14) nonetheless gives an analytic expression for the streamfunction amplitude that describes the flow surrounding a cylinder that oscillates vertically with frequency larger than the buoyancy frequency. In doing so, care must be taken in evaluating the square root of the complex argument in the denominator of (5.14) so as to ensure bounded solutions.

We now wish to find Ψ if the cylinder oscillates at frequency $\omega < N_0$. In this case the elliptic partial differential equation (5.8) becomes the hyperbolic differential equation

$$-\gamma^2\frac{\partial^2\Psi}{\partial x^2} + \frac{\partial^2\Psi}{\partial z^2} = 0, \tag{5.15}$$

in which $\gamma^2 = {N_0}^2/\omega^2 - 1 > 0$. We recognize that this is the same equation as (5.8) but with Γ replaced by $\imath\gamma$.

Through the method of analytic continuation, we can immediately solve (5.15) with boundary condition (5.9). Because we have assumed that Ψ is an analytic function, the solution (5.14) should hold whether or not Γ is real or imaginary. Thus the streamfunction amplitude is given by (5.14) in which $\Gamma = \imath\gamma$ and $Z = (-\imath x/\gamma) + \imath z$. This must be done in a way that ensures solutions are bounded and that disturbance energy propagates away from the cylinder.

Nice things happen. The argument to the square root in (5.14) becomes a real number and so the representation of Ψ explicitly in terms of real variables becomes less complicated. For this purpose, it is convenient to recast the result in terms of across-beam co-ordinates σ_+ and σ_- instead of x and z. Using the definition $|\Theta| = \cos(\omega/N_0)$, which as usual represents the magnitude of the angle formed between the vertical and lines of constant phase for waves with frequency ω, we set $\gamma = -\tan\Theta$. Here it is assumed that $\Theta < 0$ so that γ gives the (positive) slope of the wave beams in the upper right-hand and lower left-hand quadrant. (In Section 3.3.3 we saw that these waves have negative vertical and positive horizontal wavenumber if they move away from the origin, and so Θ as given by (3.56) is negative.)

Lines with slope γ are given by constant values of

$$\sigma_+ = -x\cos\Theta - z\sin\Theta. \tag{5.16}$$

Perpendicular to these are lines with constant values of

$$r_+ = -x\sin\Theta + z\cos\Theta. \tag{5.17}$$

With $\Theta < 0$, the pair (σ_+, r_+) give the across-beam and along-beam co-ordinates for waves in the first and third quadrants, as shown in Figure 5.1b.

Similarly, we define the across-beam and along-beam co-ordinates in the second and fourth quadrants by

$$\sigma_- = x\cos\Theta - z\sin\Theta \tag{5.18}$$

and

$$r_- = x\sin\Theta + z\cos\Theta, \tag{5.19}$$

respectively.

In terms of Θ, the complex co-ordinate $\mathcal{Z}$ is

$$\mathcal{Z} = -\imath\sigma_+/\sin\Theta.$$

Substituting this into (5.14) and noting that $a^2(1-1/\Gamma^2) = a^2/\sin^2\Theta$, the first term simplifies to $\Psi_+ = (1/2)Wa^2e^{-\imath\Theta}[-\sigma_+ + (\sigma_+{}^2 - a^2)^{1/2}]^{-1}$. To ensure bounded and outward-propagating solutions, the branch-cut to the square root must be taken so

that, after simplifying, we have

$$\Psi_+(x,z) = \begin{cases} \dfrac{1}{2}Wae^{-\iota\Theta}\left[-\dfrac{\sigma_+}{a} + \text{sign}\left(\dfrac{\sigma_+}{a}\right)\sqrt{\left(\dfrac{\sigma_+}{a}\right)^2 - 1}\right] & |\sigma_+/a| > 1 \\ \dfrac{1}{2}Wae^{-\iota\Theta}\left[-\dfrac{\sigma_+}{a} - \iota\sqrt{1 - \left(\dfrac{\sigma_+}{a}\right)^2}\right] & |\sigma_+/a| < 1. \end{cases} \tag{5.20}$$

This is the streamfunction amplitude for waves propagating upwards and rightwards with $r_+ > 0$ and it is assumed that $-\pi/2 < \Theta < 0$. The real and imaginary parts of Ψ_+ in the first quadrant are shown in Figure 5.3a.

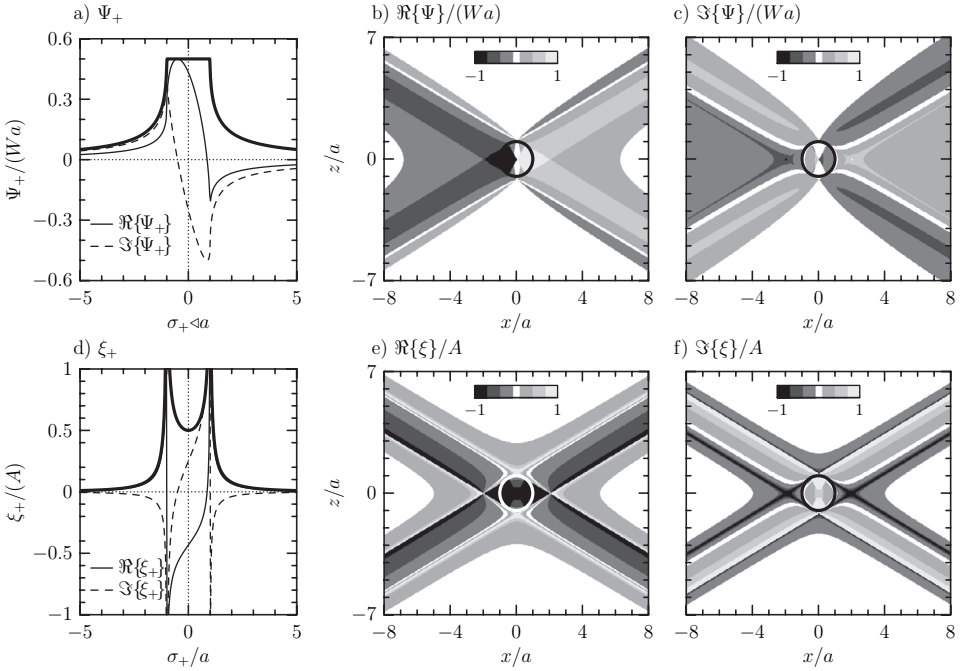

Fig. 5.3. a) Real (thin solid line), imaginary (dashed line) and magnitude (thick solid line) of the streamfunction amplitude envelope in the first quadrant, $\Psi_+(\sigma_+)$. b) Real and c) imaginary parts of the total streamfunction amplitude envelope $\Psi_+ + \Psi_-$. d) Corresponding vertical displacement field in the first quadrant, $\xi_+(\sigma_+)$ and the e) real and f) imaginary parts of the total displacement field $\xi_+ + \xi_-$. The thick circles in b), c), e) and f) indicate the location and radius of the cylinder. The real part of the field gives the flow pattern when the cylinder moves upwards through its equilibrium position (e.g. at time $t = 0$) and the imaginary part gives the flow pattern when the cylinder reaches its maximum vertical displacement (e.g. at time $t = (\pi/2)/\omega$).

There are two alternate ways of writing (5.20). Putting the σ-dependent terms in a complex exponential, we have

$$\Psi_+ = \frac{1}{2} W a e^{-\imath\Theta} \exp[-\imath \cos^{-1}(-\sigma_+/a)]. \tag{5.21}$$

The argument to the arccosine has been written as negative-valued to emphasize the necessary branch-cut to recover the second expression in (5.20). This expression makes it obvious that the magnitude of Ψ_+ is constant where $|\sigma_+| \le a$. It also reveals that the phase of the waves decreases as σ_+ increases. This is consistent with the expected downward-propagating phase (and upward-propagating energy) for waves in the first quadrant.

Using the integral transform

$$\int_0^\infty \frac{1}{k} J_\nu(k) e^{\imath k x}\, dk = \frac{1}{\nu}\Big[\sqrt{1-x^2} + \imath x\Big]^\nu, \tag{5.22}$$

(5.20) is equivalently given by

$$\Psi_+(\sigma_+) = -\imath \frac{1}{2} W a e^{-\imath\Theta} \int_0^\infty \frac{J_1(k_\sigma a)}{k_\sigma} e^{-\imath k_\sigma \sigma_+}\, dk_\sigma. \tag{5.23}$$

Here J_1 is the first-order Bessel function of the first kind. Note that the integral only sums over contributions from positive across-beam wavenumbers k_σ. The negative complex exponent in the integrand is consistent with waves in the first quadrant transporting energy upwards and so having negative wavenumber. Although the structure of the waves represented by (5.23) is less immediately apparent, this expression will prove useful later in our consideration of beam attenuation due to viscous effects.

The second term (the complex conjugate) in (5.14) is found by substituting $\Gamma = -\imath\gamma$ and simplifying as above. This gives the streamfunction amplitude Ψ_- of waves that propagate upwards and leftwards, determined so that

$$\Psi_-(\sigma_-, r_-) = -\Psi_+(\sigma_+, r_+), \tag{5.24}$$

for $r_- > 0$. By symmetry, the wave beam in the third quadrant is given by $\Psi_+(-\sigma_+, -r_+) = -\Psi_+(\sigma_+, r_+)$, and in the fourth quadrant $\Psi_-(-\sigma_-, -r_-) = -\Psi_-(\sigma_-, r_-) = \Psi_+(\sigma_+, r_+)$. Thus the streamfunction amplitude is seen to be composed of a superposition of outward-propagating beams represented by $\Psi = \Psi_+ + \Psi_-$. It is straightforward to show that Ψ satisfies the boundary condition (5.4).

Through analytic continuation, the resulting solution for Ψ is complex, the real and imaginary parts of which are plotted in Figures 5.3b and c, respectively. It is understood that the actual structure of the waves is given by the real part of (5.1). Thus Figure 5.3b represents the streamfunction as the centre of the cylinder moves

upwards through the origin and Figure 5.3c represents the streamfunction when the cylinder moves to its maximum vertical displacement a quarter-period later.

Although the streamfunction is continuous, derivatives with respect to $\sigma_\pm$ are not. In particular, (5.20) predicts that the along-beam velocity is infinite where $\sigma_\pm = a$. Likewise, the result predicts that the vertical displacement amplitude, given by $\xi = (\imath/\omega)\Psi_x$, is infinite. This field is plotted in Figure 5.3d, e and f. The approach to infinity along the tangents to the cylinder is so rapid that the integrated instantaneous mass flux is finite. Nonetheless, this counterintuitive and unphysical result reflects a deficiency in the approximations used to derive the solution. This is addressed in the next section.

5.2.2 Oscillating cylinder in viscous fluid

Primarily the singularities in the displacement and velocity field arise because we have neglected viscosity. The boundary condition (5.4) requires no-normal flow across the cylinder but does permit free-slip flow along the cylinder. Furthermore, the large across-beam variations of ψ near tangents to the cylinder imply that viscosity will act to smooth the gradients and keep the along-beam velocities and displacements finite. Thus viscosity plays a non-negligible role even for flows with very large Reynolds numbers.

The boundary value problem that includes no-slip conditions on the cylinder is difficult to solve analytically. However, the spreading of wave beams due to viscosity, an effect known as 'viscous attenuation', can be accounted for through a technique known as boundary layer theory.

In a Newtonian fluid, viscous effects are accounted for by adding the diffusion term $\mu\nabla^2\vec{u}$ to the right-hand side of the momentum equations. This has been done for a liquid in (3.37). Explicitly, in the Boussinesq approximation the momentum equations are

$$\frac{D\vec{u}}{Dt} = -\frac{1}{\varrho_0}\nabla p - \frac{1}{\varrho_0} g\rho\,\hat{z} + \nu\nabla^2\vec{u}. \tag{5.25}$$

The constant μ is the 'molecular viscosity', which effectively plays the role of friction acting within the fluid. When divided by the density ϱ_0 we have the 'kinematic viscosity' $\nu \equiv \mu/\varrho_0$. This is a measure of the diffusivity of velocity in a spatially varying shear flow. Its characteristic value for water is $\nu \simeq 10^{-6}\,\mathrm{m}^2/\mathrm{s}$ and for air is $\nu \simeq 10^{-5}\,\mathrm{m}^2/\mathrm{s}$.

For small-amplitude waves, we may combine the linearized form of the momentum equations (5.25) together with the continuity equation for an incompressible fluid (1.30) to give a single, fourth-order partial differential equation in Ψ:

$$N_0{}^2\frac{\partial^2\Psi}{\partial x^2} - \omega^2\nabla^2\Psi + \imath\omega\nu\nabla^4\Psi = 0. \tag{5.26}$$

In deriving this equation, we have included the diffusivity of momentum but we have neglected the diffusivity of salinity. Particularly in laboratory experiments performed using salt-stratified solutions, this assumption is reasonable considering that salt-diffusivity is three orders of magnitude smaller than ν.

Focusing upon the upward-propagating beam alone, we use (5.16) and (5.17) to transform (5.26) into across- and along-beam co-ordinates. We further assume that across-beam variations are more significant than along-beam variations. Thus we neglect r_+ derivatives of order two or greater in the resulting partial differential equations. This assumption is analogous to making the boundary-layer approximation for viscous flow over a rigid surface. Dropping the subscripts from σ_+, r_+ and Ψ_+, the resulting equation for the streamfunction in the first quadrant is

$$\frac{\partial^2 \Psi}{\partial \sigma \, \partial r} + \frac{\imath \nu}{2 N_0 \sin \Theta} \frac{\partial^4 \Psi}{\partial \sigma^4} = 0. \tag{5.27}$$

We anticipate that viscous effects will become increasingly important in the far field, $r \gg a$, but that the inviscid solution (5.20) adequately represents the structure near the cylinder itself. Thus an approximate solution of (5.27) can be found by Fourier transforming in σ, solving the resulting ordinary differential equation in r, inverse transforming, and matching the solution at $r = 0$ with the integral representation of the inviscid waves, (5.23). Thus we find

$$\Psi_{(\sigma)} = -\imath \frac{1}{2} W a e^{-\imath \Theta} \int_0^\infty \frac{J_1(K)}{K} \exp\left(-K^3 \tilde{\nu} \frac{r}{a} - \imath K \frac{\sigma}{a} \right) dK, \tag{5.28}$$

in which $K = k_\sigma a$ is a nondimensional measure of the across-beam wavenumber k_σ, and the nondimensional quantity

$$\tilde{\nu} = \frac{\nu}{2 a^2 N_0 \sin |\Theta|} \tag{5.29}$$

is a measure of the rate of viscous attenuation with along-beam distance away from the cylinder.

From (5.28), we may go on to find the velocity and displacement fields. In particular, the vertical displacement field $\xi(x,z)$ is given by

$$\xi = \frac{1}{-\imath \omega} \frac{\partial \Psi(x,z)}{\partial x} \simeq \frac{-\imath}{N_0} \frac{\partial \Psi(r,\sigma)}{\partial \sigma}. \tag{5.30}$$

In this last expression, we have used the dispersion relation $\omega = N_0 \cos(\Theta)$ and the boundary-layer approximation has been invoked, resulting in neglect of the $\partial_r \Psi$ term.

Figure 5.4 shows the predicted structure of upward- and rightward-propagating waves generated by an oscillating cylinder. The calculated vertical displacement

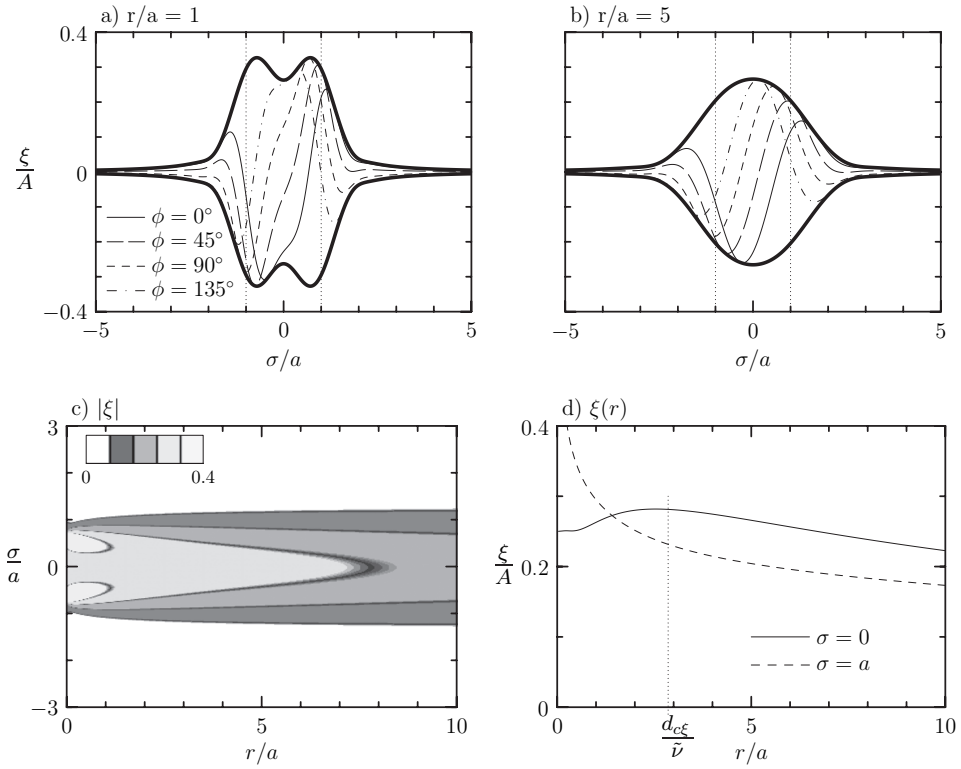

Fig. 5.4. Values of the vertical displacement field, ξ, computed in the first quadrant for a circular cylinder of radius a oscillating with relative frequency $\omega/N = 0.5$ and maximum vertical displacement $A = W/\omega$. The kinematic viscosity is set to be $\nu = 0.01a^2N$ so the effects of viscous attenuation are governed by the parameter $\tilde{\nu} \simeq 0.0058$. Instantaneous values of ξ are evaluated at along-beam distances a) $r/a = 1$ and b) $r/a = 5$. The plots show both the envelope (thick solid lines) and the instantaneous amplitude of the waves at phase $\phi = 0$ (thin solid line), $\phi = \pi/4$ (long-dashed line), $\phi = \pi/2$ (short-dashed line), $\phi = 3\pi/4$ (dashed-dotted line). The dotted vertical lines in both plots illustrate the values $\sigma = \pm a$. c) Contours of the amplitude envelope $|\xi(r,\sigma)|$ show the transition from bimodal to unimodal beams. d) Values of $|\xi|$ as a function of along-beam distance evaluated at $\sigma = 0$ (solid line) and $\sigma = a$ (dashed line). The positions $d_{\star\xi}$, where the centreline reaches maximum amplitude, and $d_{c\xi}$, where the across-beam curvature is zero, are indicated.

field is normalized by the vertical displacement A of the cylinder. The plots of the across-beam amplitude at different phases ϕ of oscillation are shown in Figures 5.4a and b. As expected for waves with upward group velocity, the phase lines move downwards (to decreasing σ) as ϕ increases. The amplitude envelope at $r = a$ exhibits two peaks near $\sigma = \pm a$. Further from the cylinder, these peaks merge as

the wave beam spreads due to viscosity. At $r = 5a$, the peak amplitude occurs along the centreline of the beam where $\sigma = 0$.

The change in structure from bimodal (having peak amplitudes on either side of the centreline of the beam) to unimodal (having peak amplitude along the centreline) is evident in the structure of the amplitude envelope of ξ, shown as a function of r and σ in Figure 5.4c. After the beam adopts a unimodal structure the centreline amplitude gradually decreases and the beam widens as r increases. This broadening and weakening of the beam due to viscosity is what is referred to as viscous attenuation.

One way to characterize the bimodal-to-unimodal transition is through the across-beam curvature of the amplitude envelope measured at the centreline. This is positive (concave upward) for bimodal beams and negative (concave downward) for unimodal beams. We define r_c to be the along-beam distance where the centreline curvature of the streamfunction amplitude envelope is zero. That is,

$$\left.\frac{\partial^2 |\Psi|}{\partial \sigma^2}\right|_{(\sigma,r)=(0,r_c)} = 0. \tag{5.31}$$

In order to evaluate r_c, we define

$$I_n(d;p) = \int_0^\infty K^{p-1} J_n(K) e^{-K^3 d}\, dK, \tag{5.32}$$

in which $d = \tilde{\nu} r/a$ with $\tilde{\nu}$ given by (5.29). Substituting (5.28) into (5.31), the condition for r_c is given through the implicit algebraic relationship

$$I_1{}^2(d_c;1) = I_1(d_c;0) I_1(d_c;2), \tag{5.33}$$

in which $d_c = \tilde{\nu} r_c/a$. The integrals in (5.32) may be evaluated numerically and from these it is found that $d_c \simeq 0.00605$.

Where the streamfunction changes from bimodal to unimodal behaviour does not necessarily occur at the same location for other fields. For example, the transition of the vertical displacement field occurs at $r_{c\xi}$ where $\partial_{\sigma\sigma}|\xi| = 0$. Using this condition together with (5.30), the transition distance is given by

$$I_1{}^2(d_{c\xi};2) = I_1(d_{c\xi};1) I_1(d_{c\xi};3). \tag{5.34}$$

Numerically, one finds that $d_{c\xi} \simeq 0.01650$, as indicated in Figure 5.4d. This is the same value computed for the transition distance of the velocity fields.

Asymptotic approximations to the integrals (5.32) can be used to determine the rate of decay of the amplitude envelopes far from the cylinder. For example, the

Table 5.1. *Theoretically predicted values of the non-dimensional along-beam distance $d_c = \tilde{\nu} r/a$ at which the across-beam curvature is zero along the centreline. Also listed are power law decay rates ($\propto r^{-p_\nu}$) of the centreline beam amplitudes as $r \to \infty$.*

field	cylinder	sphere
streamfunction: Ψ	$d_c = 0.00605$ $p_\nu = 1/3$	$d_c = 0.00507$ $p_\nu = 1$
velocity: $\vec{u}$ displacement: $\vec{\xi}$	$d_c = 0.01650$ $p_\nu = 2/3$	$d_c = 0.01086$ $p_\nu = 4/3$

streamfunction amplitude envelope along the centreline is given by evaluating (5.28) at $\sigma = 0$:

$$|\Psi|_{\sigma=0} = \frac{1}{2} Wa \int_0^\infty \frac{J_1(K)}{K} e^{-K^3 d}\, dK, \tag{5.35}$$

in which $d = \tilde{\nu} r/a$, as before.

If d is large, the integral is dominated by the behaviour of the integrand for small K. This inspires us to perform a Taylor-series expansion of the first-order Bessel function about $K = 0$: $J_1 \simeq K/2$. The integration variable K in the resulting approximation can be replaced by $\tilde{K} = dK^3$ and so the definite integral is converted into the form of a Gamma function. Explicitly we find

$$|\Psi|_{\sigma=0} = \frac{1}{6} \Gamma(1/3) Wa\, d^{-1/3} \propto r^{-1/3}. \tag{5.36}$$

And so we have found that the amplitude decreases as the negative one-third power of the distance far from the cylinder along the centreline of the beam.

Likewise we can compute the power law rate of decay, r^{-p_ν}, for other fields of interest. The power law exponents, p_ν, are listed in Table 5.1. In particular, for the displacement and velocity fields, we find $p_\nu = 2/3$, meaning that the amplitudes of these fields decay with distance more rapidly than the streamfunction.

5.2.3 Oscillating sphere

The analysis of internal waves generated by an oscillating sphere is similar to that for an oscillating cylinder. However, there are significant qualitative differences in the resulting predictions that the circumstance is worth considering here in some detail.